−1 to 1), and MTX. Desired neutrophil counts (>500 per μL) were obtained by day 11, reticulocyte counts (>1.0 %) by day 12, and platelet counts (>5.0 × 10^4 per μL) by day 18. Stage 1 acute GVHD and limited chronic GVHD of the skin have been observed. He remains in CR at 18 months after his second allo-HSCT.

To identify additional genetic alterations at relapse, a comprehensive genomic analysis of leukemic cells at the initial diagnosis and at the time of relapse was performed. Informed consent was obtained from his parents according to the Declaration of Helsinki. First, genome-wide analysis for genetic lesions was performed by single nucleotide polymorphism (SNP) array analysis using the Affymetrix Genome-Wide Human SNP 6.0 array (Affymetrix, Santaclala, CA, USA). The data obtained were processed using CNAG software (http://www.genome.umin.jp). SNP array analysis detected acquired losses at 2q14.1–q14.3, 5q31.1, 13q13.3–q14.1, 13q14.2–q21.1, and 13q21.1–q21.3, and UPD at the 19p13.3–p12 locus, only in leukemic cells at relapse (Table 1). Because ETP-ALL has been reported to be characterized by activating mutations in genes regulating cytokine receptors and RAS signaling (67 % of cases; *NRAS, KRAS, FLT3, IL7R, JAK3, JAK1, SH2B3*, and *BRAF*) [2], we focused on the UPD at 19p13.3–p12, where the *JAK3* gene is located (Fig. 1a, b). Thus, direct sequence of *JAK3* was performed. The entire coding region of the *JAK3* was amplified by RT-PCR using the primers listed in supplemental Table 1. Then, the PCR products were sequenced using Big Dye Terminator Sequencing Kit (Applied Biosystem, Darmstadt, Germany). Direct sequencing of the *JAK3* gene revealed that a hemizygous *JAK3* V674A mutation was present in leukemic cells at diagnosis (Fig. 1c). Interestingly, direct sequencing of the *JAK3* gene revealed the loss of normal allele (Fig. 1d). Considering UPD at 19p13.3–p12, *JAK3* V674A was homozygous at relapse.

Next, we performed whole-exome sequence (WES) of the paired samples in this case. The procedure of WES is same as previously described [5]. Briefly, exome capture was performed using SureSelect Human All Exon V5, and enriched exome fragments were then subjected to massively parallel sequencing using HiSeq 2000 platform (Illumina). The mean depth of WES was 129, 90, and 101 for the diagnostic, relapsed, and reference specimens,

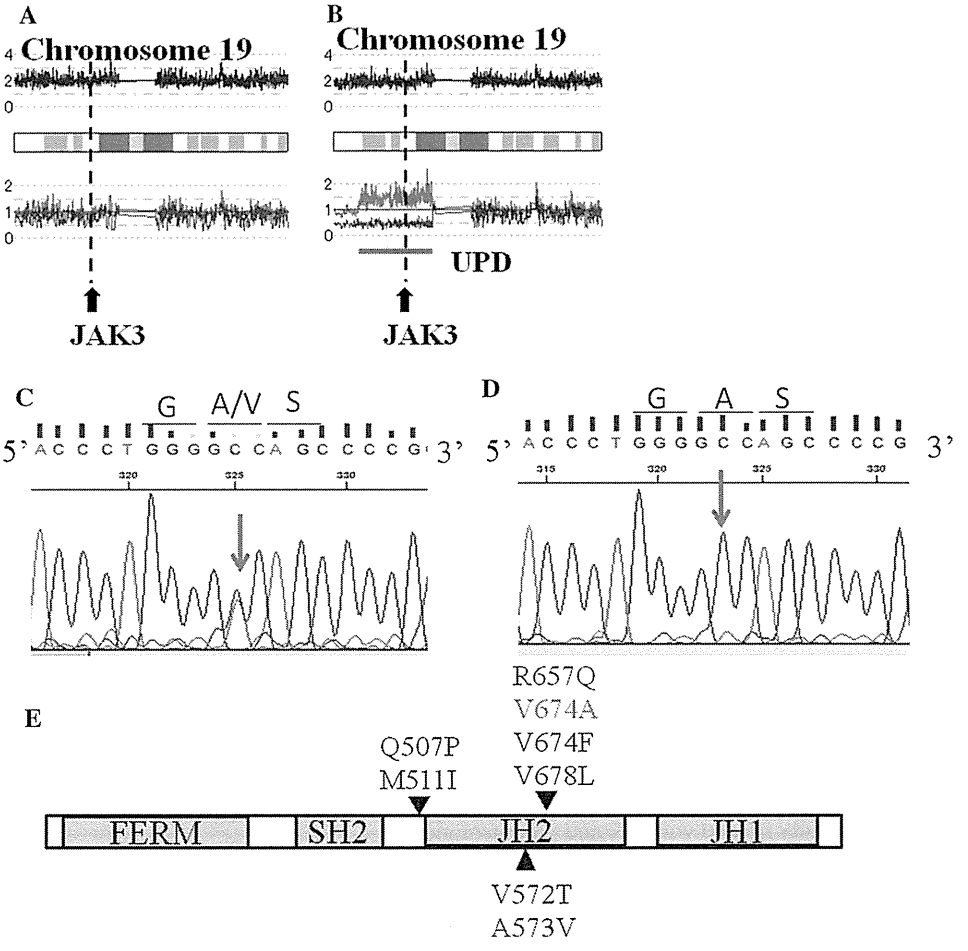

Fig. 1 Results of a single nucleotide polymorphism (SNP) array analysis for leukemic cells at initial diagnosis (**a**) and relapse (**b**). The *blue line* shows the total gene dosage. The *green* and *red lines* show allele-specific gene dosage levels. Uniparental disomy (UPD) at the 19p13.3–p12 locus was detected at relapse (*brown line*), whereas UPD was absent at initial diagnosis. Results of direct sequencing for the *JAK3* gene in leukemic cells at initial diagnosis (**c**) and relapse (**d**). **e** Primary structure of JAK3 showing the location of the point mutation (V674A). V674A mutation was previously reported only in two T-ALL patients. FERM, band 4.1 ezrin, radixin, and moesin domain; SH2, src homology domain; JH2, pseudokinase domain; and JH1, kinase domain

Table 2 The list of mutated genes in diagnostic and relapsed samples in whole-exome sequencing

Sample	Gene	Amino acid change	Nucleotide change	Variant frequency
Relapse	*AHNAK2*	p.V1222I	c.G3664A	0.375
Diagnosis	*AHNAK2*	p.V1222I	c.G3664A	0.520408163
Relapse	*ARHGEF10L*	p.R674C	c.C2020T	0.536585366
Diagnosis	*ARHGEF10L*	p.R674C	c.C2020T	0.566037736
Relapse	*ATP1B4*	p.R280X	c.C838T	0.8
Diagnosis	*ATP1B4*	p.R280X	c.C838T	0.873015873
Relapse	*GALNTL6*	p.G26A	c.G77C	0.355263158
Diagnosis	*GALNTL6*	p.G26A	c.G77C	0.464285714
Relapse	*GATA3*	p.R276Q	c.G827A	0.84057971
Diagnosis	*GATA3*	p.R276Q	c.G827A	0.897435897
Relapse	*JAK3*	p.V674A	c.T2021C	0.89189189
Diagnosis	*JAK3*	p.V674A	c.T2021C	0.41558442
Relapse	*LAMA1*	p.R1180C	c.C3538T	0.344262295
Diagnosis	*LAMA1*	p.R1180C	c.C3538T	0.472
Relapse	*LILRB5*	p.A104 V	c.C311T	0.295081967
Diagnosis	*LILRB5*	p.A104 V	c.C311T	0.4
Relapse	*MMP3*	p.R110S	c.G330T	0.315789474
Diagnosis	*MMP3*	p.R110S	c.G330T	0.514084507
Relapse	*MYB*	p.W82R	c.T244A	0.353846154
Diagnosis	*MYB*	p.W82R	c.T244A	0.415662651
Relapse	*MYO5B*	p.C798F	c.G2393T	0.53030303
Diagnosis	*MYO5B*	p.C798F	c.G2393T	0.473684211
Relapse	*NCOR1*	p.E1345X	c.G4033T	0.469798658
Diagnosis	*NCOR1*	p.E1345X	c.G4033T	0.709803922
Relapse	*NOTCH1*	p.Q2391X	c.C7171T	0.454545455
Diagnosis	*NOTCH1*	p.Q2391X	c.C7171T	0.395522388
Relapse	*OR52K1*	p.R302H	c.G905A	0.489655172
Diagnosis	*OR52K1*	p.R302H	c.G905A	0.470899471
Relapse	*PIDD*	p.A499T	c.G1495A	0.339285714
Diagnosis	*PIDD*	p.A499T	c.G1495A	0.421052632
Relapse	*RPTN*	p.G159S	c.G475A	0.116731518
Diagnosis	*RPTN*	p.G159S	c.G475A	0.105960265
Diagnosis	*ARVCF*	p.N5D	c.A13G	0.578947368
Diagnosis	*DMKN*	p.G271S	c.G811A	0.636363636
Diagnosis	*KRT24*	p.N222 K	c.T666A	0.571428571
Diagnosis	*MUC17*	p.T1541P	c.A4621C	0.148479428
Diagnosis	*NOTCH1*	p.I1718T	c.T5153C	0.449704142
Diagnosis	*PRDM9*	p.R842S	c.C2524A	0.153153153
Diagnosis	*ST5*	p.R478 W	c.C1432T	0.37
Relapse	*AIRE*	p.G8R	c.G22A	0.373913043
Relapse	*AP1G1*	p.Q470P	c.A1409C	0.423423423
Relapse	*CASP5*	p.R23 fs	c.67delA	0.14953271
Relapse	*CSMD3*	p.L1821F	c.G5463T	0.374301676
Relapse	*DSCAM*	p.R1624 M	c.G4871T	0.368421053
Relapse	*FRG1*	p.R128C	c.C382T	0.072
Relapse	*JAK1*	p.E1012G	c.A3035G	0.157894737
Relapse	*L2HGDH*		exon5:c.409-1G > T	0.333333333
Relapse	*LIMA1*	p.V54F	c.G160T	0.538461538
Relapse	*MIER2*		exon11:c.984 + 1G > T	0.289719626
Relapse	*MMP27*		exon4:c.490 + 1G > C	0.379746835

Table 2 continued

Sample	Gene	Amino acid change	Nucleotide change	Variant frequency
Relapse	*N4BP2L2*	p.M549I	c.G1647T	0.368421053
Relapse	*SF3A2*	p.A385T	c.G1153A	0.909090909
Relapse	*SLC23A2*	p.M57I	c.G171A	0.444444444
Relapse	*SNX10*	p.R10C	c.C28T	0.201834862
Relapse	*SPEG*	p.W243L	c.G728T	0.355555556
Relapse	*SYNJ1*	p.L1320 M	c.T3958A	0.333333333
Relapse	*ZFR*	p.V181A	c.T542C	0.474576271

The mutations of the listed genes except for *JAK3* were not validated by other analysis, such as the targeted deep sequencing and/or Sanger sequencing

respectively. More than 90 % of the targeted exons were analyzed by more than 30 independent reads (96.3 % for diagnostic, 91.1 % for relapsed, and 94.8 % for reference specimens, respectively).

The buccal cells were used as normal control. The result was summarized in Table 2. There were 16 genes which were mutated both in diagnostic and relapsed samples and included essential transcriptional factors related to T-ALL, such as *GATA3*, *MYB* and *NOTCH1* [2, 6]. Interestingly, *JAK3* V674A mutation was identified in both samples and the frequency was almost double in relapsed sample, which was consistent with the result of SNP array analysis. Although the results of WES were not validated by Sanger sequencing and/or targeted deep sequencing, there were 7 and 18 genes only in diagnostic and relapsed samples, respectively. *JAK1* E1012G was identified only in relapsed samples with low frequency, suggesting this mutation was not associated with the relapse. To the best of our knowledge, there was no genetic alteration which was known to be associated with T-ALL in 18 mutated genes found only in relapsed samples. These findings suggested that homozygous *JAK3* mutation was potentially associated with the relapse in this case.

Discussion

JAK3 is a cytoplasmic tyrosine kinase that plays an important role in T-cell development and function [7, 8]. Recently, mutations of pseudokinase domain of *JAK3* including V674A have been identified in T cell leukemia (Fig. 1e) [2, 9, 10]. Bergmann et al. [10] indicated V674A could increase kinase activity by disrupting the activation loop and the interface between N and C lobes, increasing the accessibility of the catalytic loop. Indeed, Choi et al. [3] demonstrated that 32D cells expressing *JAK3* V674A grew in the absence of cytokine, showing that the *JAK3* V674A mutation abrogates the cytokine dependency of 32D cells. These findings suggest that *JAK3* V674A contributes to leukemogenesis and could be a therapeutic target.

Raghavan et al. [11] reported that approximately 40 % of patients with acute myeloid leukemia (AML) exhibit a newly acquired UPD at relapse, and an acquired UPD frequently results in a homozygous mutation, most commonly internal tandem duplications (ITDs) of *FLT3* on chromosome 13. This suggests that mitotic recombination is an important mechanism responsible for recurrence of AML. As described above, ETP-ALL is characterized by activating mutations in genes regulating cytokine receptors and RAS signaling, such as JAK3 [2]. In this ETP-ALL patient, we identified a newly acquired UPD at relapse, resulting in a homozygous *JAK3* V674A mutation. In addition, WES of paired samples identified 18 genes mutated only in relapsed sample. Although there is the possibility that some of these 18 mutated genes are associated with the relapse, none of them except for *JAK1* was known to be associated with T-ALL. These findings suggest homozygous *JAK3* V674A mutation might be deeply associated with the relapse in this case. Further genetic analysis of more patients with paired leukemic samples is required to assess the contribution of not only UPD of *JAK3* mutation, but also other genetic alterations to the relapse of ETP-ALL.

Conflict of interest The authors report no potential conflicts of interest

References

1. Coustan-Smith E, Mullighan CG, Onciu M, Behm FG, Raimondi SC, Pei D, et al. Early T-cell precursor leukemia: a subtype of very high-risk acute lymphoblastic leukemia. Lancet Oncol. 2009;10:147–56.
2. Zhang J, Ding L, Holmfeldt L, Wu G, Heatley SL, Payne-Turner D, et al. The genetic basis of early T-cell precursor acute lymphoblastic leukemia. Nature. 2012;481:157–63.
3. Choi YL, Kaneda R, Wada T, Fujiwara S, Soda M, Watanabe H, et al. Identification of a constitutively active mutant of JAK3 by retroviral expression screening. Leuk Res. 2007;31:203–9.
4. Suzuki N, Yumura-Yagi K, Yoshida M, Hara J, Nishimura S, Kudoh T, et al. Outcome of childhood acute lymphoblastic leukemia with induction failure treated by the Japan Associated of Childhood Leukemia study (JACLS) ALL F-protocol. Pediatr Blood Cancer. 2010;54:71–8.
5. Yoshida K, Toki T, Okuno Y, Kanezaki R, Shiraishi Y, Sato-Otsubo A, et al. The landscape of somatic mutations in Down syndrome-related myeloid disorders. Nat Genet. 2013;45:1293–9.

6. Lahortiga I, De Keersmaecker K, Van Vlierberghe P, Graux C, Cauwelier B, Lambert F, et al. Duplication of the MYB oncogene in T cell acute lymphoblastic leukemia. Nat Genet. 2007;39:593–5.
7. Witthuhn BA, Silvenoinen O, Miura O, Lai KS, Cwik C, Liu ET, et al. Involvement of the JAK-3 Janus kinase in signaling by interleukins 2 and 4 in lymphoid and myeloid cells. Nature. 1994;370:153–7.
8. Macchi P, Villa A, Giliani S, Sacco MG, Frattini A, Porta F, et al. Mutations of Jak-3 gene in patients with autosomal severe combined immune deficiency (SCID). Nature. 1995;377:65–8.
9. Kalender Atak Z, De Keerskaecker K, Gianfelici V, Geerdens E, Vandepoel R, Pauwels D, et al. High accuracy mutation detection in leukemia on a selected panel of cancer genes. PLoS One. 2012;7:e38463.
10. Bergmann AK, Schneppenheim S, Seifert M, Betts MJ, Haake A, Lopez C, et al. Recurrent mutation of JAK3 in T-cell prolymphocytic leukemia. Genes Chromosomes Cancer. 2014;53:309–16.
11. Raghavan M, Smith LL, Lilllington DM, Chaplin T, Kakkas I, Molloy G, et al. Segmental uniparental disomy is a commonly acquired genetic event in relapsed acute myeloid leukemia. Blood. 2008;112:814–21.

GENES, CHROMOSOMES & CANCER 53:299–308 (2014)

The Leucine Twenty Homeobox (*LEUTX*) Gene, Which Lacks a Histone Acetyltransferase Domain, is Fused to *KAT6A* in Therapy-Related Acute Myeloid Leukemia with t(8;19)(p11;q13)

Yoshiaki Chinen,[1] Tomohiko Taki,[2] Yasuhiko Tsutsumi,[1] Satoru Kobayashi,[1] Yosuke Matsumoto,[1] Natsumi Sakamoto,[1] Junya Kuroda,[1] Shigeo Horiike,[1] Kazuhiro Nishida,[1] Hirofumi Ohno,[3] Naokuni Uike,[3] and Masafumi Taniwaki[1]*

[1]Department of Molecular Hematology and Oncology, Kyoto Prefectural University of Medicine Graduate School of Medical Science, Kyoto, Japan
[2]Department of Molecular Diagnostics and Therapeutics, Kyoto Prefectural University of Medicine Graduate School of Medical Science, Kyoto, Japan
[3]Department of Hematology, National Kyushu Cancer Center, Fukuoka, Japan

The monocytic leukemia zinc finger protein *KAT6A* (formerly *MOZ*) gene is recurrently rearranged by chromosomal translocations in acute myeloid leukemia (AML). *KAT6A* is known to be fused to several genes, all of which have histone acetyltransferase (HAT) activity and interact with a number of transcription factors as a transcriptional coactivator. The present study shows that the leucine twenty homeobox (*LEUTX*) gene on 19q13 is fused to the *KAT6A* gene on 8p11 in a therapy-related AML with t(8;19)(p11;q13) using the cDNA bubble PCR method. The fusion transcripts contained 83 nucleotides upstream of the first ATG of *LEUTX* and are presumed to create in-frame fusion proteins. *LEUTX* is known to have a homeobox domain. Expression of the *LEUTX* gene was only detected in placenta RNA by RT-PCR, but not in any tissues by Northern blot analysis. The putative LEUTX protein does not contain any HAT domain, and this is the first study to report that *KAT6A* can fuse to the homeobox gene. The current study, with identification of a new partner gene to *KAT6A* in a therapy-related AML, does not elucidate the mechanisms of leukemogenesis in *KAT6A*-related AML but describes a new gene with a different putative function.

INTRODUCTION

Several leukemias are genetically characterized by the presence of acquired translocations and inversions that result in fusion genes of pathogenetic, diagnostic, and prognostic importance. The 8p11 translocations result in diverse oncogenic fusion genes involving fibroblast growth factor receptor 1 (*FGFR1*) or monocytic leukemia zinc finger protein (*KAT6A*, previously *MOZ* or *MYST3*). *FGFR1* encodes a receptor tyrosine kinase, rearrangements of which have been associated with stem cell leukemia/lymphoma or myeloproliferative neoplasm, whereas *KAT6A* is a member of a histone acetyltransferase family associated with monoblastic and monocytic leukemia (Patnaik et al., 2010). *KAT6A*-related translocations are associated with the same type of acute myeloid leukemia (AML), with blast cells of a monocytoid phenotype having pronounced erythrophagocytic activity. This subtype is found in ~2% of cases of AML with the French-American-British classification M4 or M5 phenotype (Aguiar et al., 1997). The most frequent translocation partner gene for *KAT6A* is *CREBBP* in t(8;16)(p11.2;p13.3) (Borrow et al., 1996), other 8p11 translocations involving *KAT6A* give rise to fusion oncogenes such as *KAT6A-NCOA2* (nuclear receptor coactivator 2, also known as *TIF2* or *GRIP1*) in inv(8)(p11q13) (Liang et al., 1998),

Supported by: a research program of the Project for Development of Innovative Research on Cancer Therapeutics (P-Direct) and a Grant-in-Aid for Scientific Research (C) from the Ministry of Education, Culture, Sports, Science and Technology of Japan.

*Correspondence to: Masafumi Taniwaki MD, PhD, Department of Molecular Hematology and Oncology, Kyoto Prefectural University of Medicine Graduate School of Medical Science, 465 Kajii-cho, Kawaramachi-hirokoji, Kamigyo-ku, Kyoto 602-8566, Japan. E-mail: taniwaki@koto.kpu-m.ac.jp

Received 13 August 2013; Accepted 5 December 2013
DOI 10.1002/gcc.22140
Published online 21 January 2014 in Wiley Online Library (wileyonlinelibrary.com).

KAT6A-EP300 (adenoviral EIA-associated protein *p300*) in t(8;22)(p11;q13) (Chaffanet et al., 2000), and *KAT6A-NCOA3* (nuclear receptor coactivator 3, also known as *TRAM-1*, *RAC3*, *pCIP*, or *AIB-1*) in t(8;20)(p11;q13) (Esteyries et al., 2008). These fusion genes produce the same disease pattern with blast cells of a monocytoid phenotype. Previous studies have revealed that *KAT6A* is essential for the self-renewal of hematopoietic stem cells (Katsumoto et al., 2006; Thomas et al., 2006), and KAT6A fusion proteins enable the transformation of non-self-renewing myeloid progenitors into leukemia stem cells (Huntly et al., 2004). Other data have shown that *KAT6A* cooperates with *MLL* to regulate *HOX* gene expression in human cord blood CD34+ cells (Paggetti et al., 2010). In the present study, a case of therapy-related AML with t(8;19)(p11;q13) was analyzed and a novel *KAT6A* fusion partner was identified using the cDNA bubble PCR method.

MATERIALS AND METHODS

Patient

A 71-year-old male was initially diagnosed as having non-Hodgkin's lymphoma (diffuse large B-cell lymphoma, DLBCL, stage IIIA, IPI: high-intermediate). He was treated with six cycles of chemotherapy consisting of R-THP-COP (rituximab, pirarubicin, cyclophosphamide, vincristine, and prednisolone), after which partial remission was obtained. Six months after treatment initiation, he presented to the hospital complaining of general malaise and dyspnea. Complete blood cell count on admission demonstrated elevated white blood cell count (6.62×10^9/l, 44% blast) and thrombocytopenia (46×10^9/l). Bone marrow aspirate showed 78.4% blast cells, and cytochemical studies revealed that the blast cells were positive for myeloperoxidase, non-specific esterase (butyrate esterase), and specific esterase (chloroacetate esterase). He was diagnosed as having AML (FAB M4). Flow cytometric study also revealed that the vast majority of leukemic cells were positive for CD4, CD13, CD33, CD56, and HLA-DR, and high serum and urine lysozyme levels were observed (28.9 mg/l and 0.4 mg/l, respectively). These findings were also consistent with AML (FAB M4). Erythrophagocytosis was observed in bone marrow smears; however, extramedullary involvement was not observed. Other significant laboratory data included elevated lactate dehydrogenase (LDH) of 2,093 IU/l, fibrin degradation product (FDP) of 21.6 μg/ml, and D-dimer of 16.9 ng/ml, which suggested disseminated intravascular coagulation (DIC). The patient did not respond to induction chemotherapy with idarubicin and cytarabine, but responded partially to second line therapy with gemtuzumab ozogamicin. However, he died four months after the diagnosis of AML because of leukemia progression. After informed consent was obtained from the patient, the leukemic cells at diagnosis were analyzed. The Institutional Review Board of Kyoto Prefectural University of Medicine approved this study.

Spectral Karyotyping Analysis

Spectral karyotyping (SKY) analysis was performed with a Sky Painting kit (Applied Spectral Imaging, MigdalHa'Emek, Israel). Signal detection was performed according to the manufacturer's instructions.

Fluorescence In Situ Hybridization Analysis

Fluorescence in situ hybridization (FISH) analysis using *KAT6A*-specific BAC clones (RP11–45I11, 3′ of *KAT6A* and RP11–589C21, 5′ of *KAT6A*) was carried out as previously described (Taniwaki et al., 1994).

cDNA Bubble PCR

cDNA bubble PCR was conducted as previously described (Chinen et al., 2008), and its outline is shown in Figure 1. The sequences of all primers used in this study are listed in Table 1. Nested PCR was performed using the primers NVAMP-1 (bubble oligo) and MOZ-E16-1S for first-round PCR, and NVAMP-2 (bubble oligo) and MOZ-E16-2S for nested PCR. Poly(A)+ RNA was extracted from the patient's leukemic cells using the QuickPrep Micro mRNA Purification Kit (GE Healthcare, Waukesha, WI).

Bubble PCR of Genomic DNA

Bubble PCR of genomic DNA was performed as previously described (Smith, 1992; Zhang et al., 1995). Primers used were as follows: NVAMP-1 and MOZ-GNM2S1 for first-round PCR, and NVAMP-2 and MOZ-GNM2S2 for second-round PCR (Table 1).

RT-PCR and Genomic PCR Analyses

RT-PCR and genomic PCR analyses were performed as previously described (Chinen et al.,

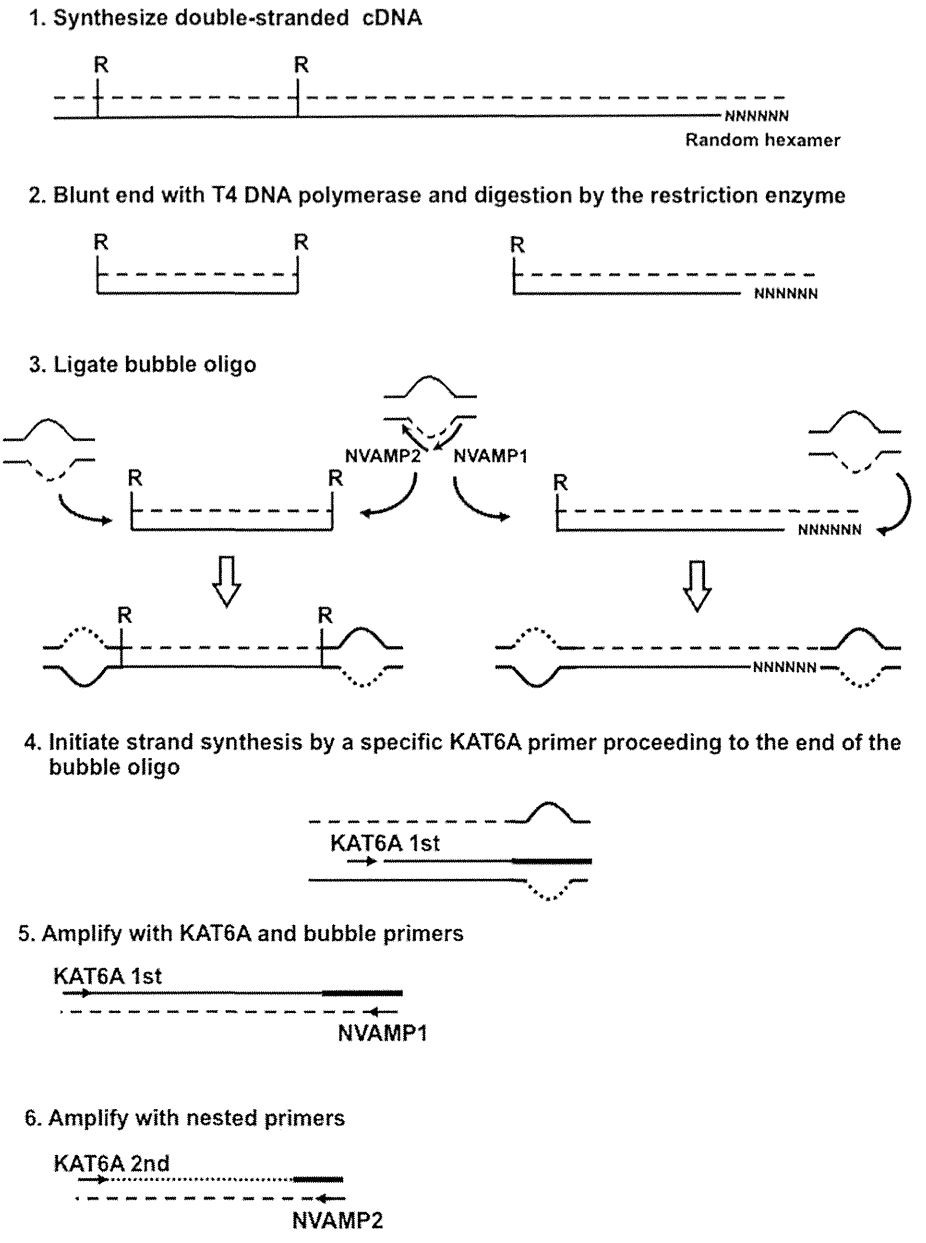

Figure 1. Outline of cDNA bubble PCR. Bubble PCR primers (NVAMP-1 and NVAMP-2) can only anneal with one complementary sequence for bubble oligo synthesized with *KAT6A* primer but not bubble oligo itself; therefore, this single-stranded bubble provides the specificity of the reaction. The sequences of primers used are listed in Table 1. Nested PCR was performed using primers NVAMP-1 (bubble oligo) and MOZ-E16-1S for 1st round PCR, and NVAMP-2 (bubble oligo) and MOZ-E16-2S for nested PCR for the detection of *KAT6A-LEUTX* fusion transcripts, and primers NVAMP-1 and MOZ-GNM2S1 for 1st round PCR, and NVAMP-2 and MOZ-GNM2S2 for nested PCR for the detection of *KAT6A-LEUTX* genomic fusion point. NVAMP1 and NVAMP2 can only anneal to the newly synthesized unique sequence of the bubble oligo by MOZ-E16-1S.

2008). After 35 rounds of PCR (30 s at 94°C, 30 s at 55°C, and 1 min at 72°C), 5 μl of PCR product was electrophoresed in a 3% agarose gel. Primer pairs were as follows: MOZ-E16-1S/MF19-1AS and MOZ-3A/MF19-1S for RT-PCR; MOZ-GNM2S2/MF19-GNM2A and MF19-GNM2S/MOZ-GNM2A for genomic PCR; MOZ-E16-1S/LEUTX-5A for RT-PCR to detect whole sequence of *LEUTX* in the chimeric transcript (Table 1).

Nucleotide Sequencing

Nucleotide sequences of PCR products and, if necessary, subcloned PCR products were analyzed as previously described (Chinen et al., 2008).

Expression Analysis of LEUTX *in Normal Tissues*

Pre-made Northern blots (human 12 lane MTN blot, Clontech, Palo Alto, CA) were hybridized to probes labeled using the Dig-labeled PCR method according to the manufacturer's instructions (Roche Applied Science, Gilroy, CA). Probes were 112 bp *LEUTX* cDNA fragments (nucleotides 166–667; GenBank accession no. NM_001143832). Human 1st strand cDNA Mix was used for RT-PCR (Genostaff, Tokyo, Japan).

TABLE 1. Primers Used in This Study

Forward primers	
MOZ-E16-1S	GGTGTCAGTCCTCTTCTAAG
MOZ-E16-2S	GATGAAGAGTCAGATGATGCTG
MOZ-GNM2S1	CCCTGATTAAGTTCCCATGG
MOZ-GNM2S2	TTGCTGATGCAGCCATTTCC
MF19-1S	CACACGGTTTTCAGCCTCAT
MF19-GNM2S	TCCCTTCAGTCTCTCACCCA
Reverse primers	
MF19-1AS	AGTCTCCTCCTTCTTCACTG
MOZ-3A	GCGTCATTGAGCCCATCGTTTCCA
MF19-GNM2A	CCAGTGGCAGAACAGTGAAT
MOZ-GNM2A	TACTCTAGGCCATGACTGAG
LEUTX-5A	TTACACTGAAGATTGGAGCTGG
Bubble PCR primers	
NVAMP1	TGCTCGTAGTAATCGTTCGCAC
NVAMP2	GTTCGCACGAGAATCGCAAGAT

RESULTS

Identification of the KAT6A-LEUTX *Fusion Transcript*

G-banding of the leukemic cells of the patient revealed 46,XY,t(8;19)(p11;q13) in all 20 cells analyzed, and it was confirmed by SKY (Fig. 2A). Because the patient was diagnosed as having AML-M4 with hemophagocytosis, and not a myeloproliferative neoplasm, a *KAT6A* rearrangement was thought more likely than an *FGFR1* rearrangement. FISH analysis using *KAT6A*-specific BAC clones

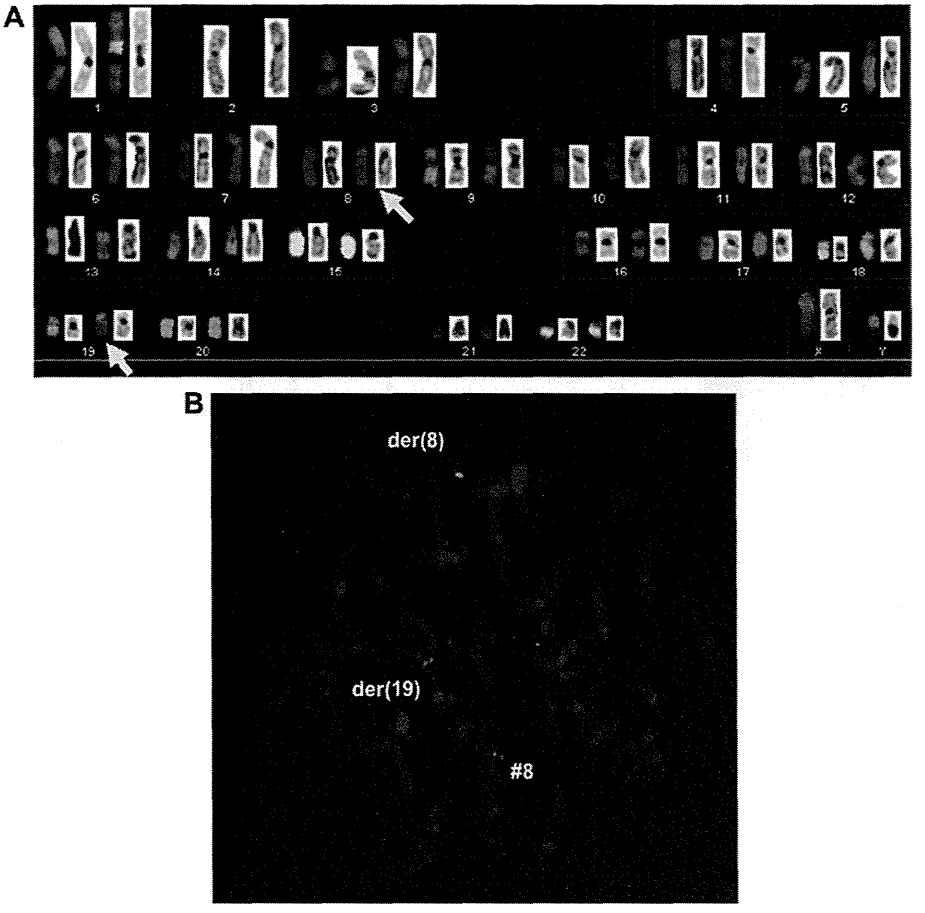

Figure 2. A: SKY analysis. Arrows indicate rearranged chromosomes. B: FISH analysis. RP11–589C11 (green, 3′ side of *KAT6A*) and RP11–45I11 (red, 5′ side of *KAT6A*). One fusion signal was detected on chromosome 8.

showed *KAT6A* split signals on der(8) and der(19) (Fig. 2B). The cDNA bubble PCR method was performed to identify the *KAT6A* fusion partner. Products of various sizes were obtained (Fig. 3A), and one product contained a 25 bp *KAT6A* sequence fused to an 84 bp unknown sequence (Fig. 3B). Initially, a BLAST search revealed that the unknown sequence was identical to that of a gene encoding a hypothetical protein identified from a human placenta cDNA library (GenBank accession no. CR746510); later, that sequence was shown to be part of the *LEUTX* (leucine twenty homeobox) gene (GenBank accession no. NR_003931). RT-PCR confirmed the in-frame fusion transcript of the exon 16 of *KAT6A* and exon 2 of *LEUTX* (Fig. 3C). The NCBI database showed that the *LEUTX* gene consists of three exons; however, the predicted amino acid sequence of *LEUTX* exon 1 continues in frame into exon 2 (Fig. 4). Although we attempted to find upstream *LEUTX* sequences, no upstream exon could be identified by bubble PCR. Another RT-PCR to detect the fusion transcripts contained whole sequence from exon 2 and to the stop codon of exon 3 were amplified (Fig. 3D).

Detection of KAT6A-LEUTX *Genomic Junctions*

To isolate the fusion point of chromosomes 8 and 19, bubble PCR was performed on genomic DNA previously digested with *Hae*III, and nested PCR products were detected using the primers MOZ-GNM2S2 and NVAMP2 (Fig. 5A). Sequence analysis of the subcloned PCR product revealed the genomic junction of 5′-*KAT6A-LEUTX*−3′, and the result was confirmed by PCR analysis using the primers MOZ-GNM2S2 and MF19-GNM2A (Fig. 5B). Bubble PCR on genomic DNA revealed that the genomic breakpoints were within intron 16 of *KAT6A* and 4,314 bp upstream of the known first exon of *LEUTX* (Fig. 5C). The fusion products of exon 1 of *LEUTX* and exon 16 of *KAT6A* were not detected by RT-PCR.

Expression of the LEUTX *Gene*

To examine the expression of the *LEUTX* gene at the RNA level, Northern blot analysis was performed using the *LEUTX* cDNA probe spanning exons 2–3. *LEUTX* RNA could not be detected in 12 various human tissues (including brain, heart, skeletal muscle, colon, thymus, spleen, kidney,

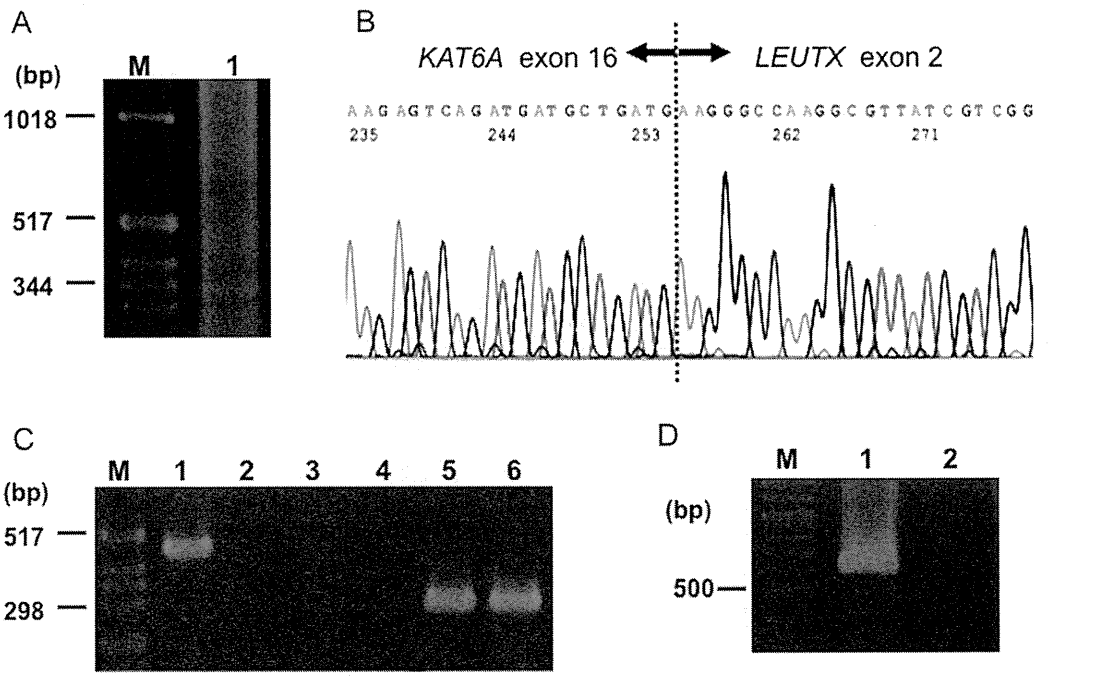

Figure 3. Identification of *KAT6A-LEUTX* fusion transcript. A: Bubble PCR products by nested PCR using MOZ-E16-1S and NVAMP1 for the 1st PCR, and MOZ-E16-2S and NVAMP2 for the 2nd PCR (lane 1). M, size marker. B: Sequence analysis of *KAT6A-LEUTX* fusion transcript. C: Detection of *KAT6A-LEUTX* fusion transcripts by RT-PCR. Primers used are: MOZ-E16-1S and MF19-1AS for 5′-*KAT6A-LEUTX*−3′ (lanes 1 and 2); MF19-1S and MOZ-3A for reciprocal fusion transcripts (lanes 3 and 4), and primers for β-actin (lanes 5 and 6). Lanes 1, 3, and 5, patient's leukemic cells; lanes 2, 4, and 6, normal peripheral lymphocytes. D: Detection of *KAT6A-LEUTX* fusion transcripts with a primer containing the stop codon of *LEUTX* by RT-PCR. Primers used are: MOZ-E16-1S and LEUTX-5A. Lane 1, patient's leukemic cells; lane 2, water; M, size marker.

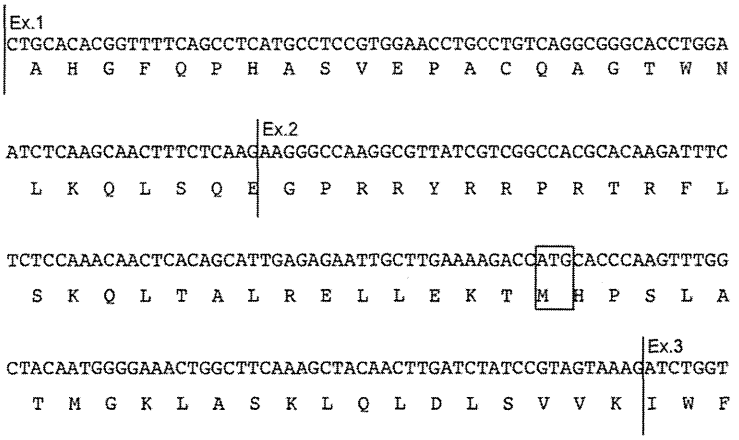

Figure 4. Partial sequencing of *LEUTX* cDNA. The NCBI database (GenBank accession no. NR_003931) shows that the *LEUTX* gene consists of three exons, and that the boxed ATG in exon 2 is the translation initiation codon of *LEUTX*; however, the frame is open all of the way to 5′ end of exon 1. Although we attempted to find upstream *LEUTX* sequences, no sequences could be identified by bubble PCR.

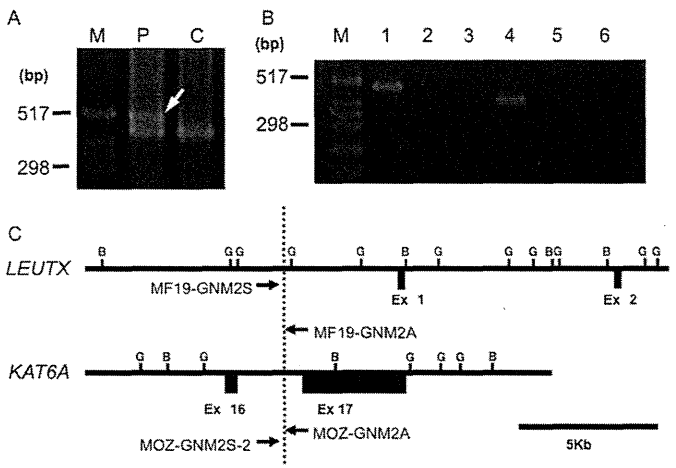

Figure 5. Cloning of the genomic junction of *KAT6A* and *LEUTX*. A: Bubble PCR for genomic DNA. P, patient's leukemic cells; N, normal peripheral lymphocytes. B: Detection of the genomic fusion point of *KAT6A-LEUTX* by PCR. Primers used are MOZ-GNM2S-2 and MF19-GNM2A (lanes 1–3), and MF19-GNM2S and MOZ-GNM2A (lanes 4–6). Lanes 1 and 4, patient's leukemic cells; lanes 2 and 5, leukemic cell line PEER; lanes 3 and 6, water. M, size marker. C: Physical map of the breakpoint regions. Black boxes represent defined exons in each gene. Horizontal arrows show the primers used. Restriction sites are indicated by capital letters: G, *Bgl*II; B, *Bam*HI.

liver, small intestine, placenta, lung, and peripheral blood leukocytes). RT-PCR with the human cDNA mix with 12 tissues (including brain, heart, liver, lung, kidney, stomach, small intestine, large intestine, muscle, spleen, placenta, and testis) also could not detect any *LEUTX* gene transcript. Since the NCBI expressed sequence tag (EST) database showed that *LEUTX* was expressed only in placenta, RT-PCR was performed using human placental total RNA (Clontech, Palo Alto, CA) as template, which finally revealed the normal *LEUTX* transcript. No expression of the *LEUTX* transcript was found in any leukemic cell line, such as Kasumi-3, ML-1, LAZ-22, TS 9;22, or THP-6 (data not shown).

DISCUSSION

This study identified a novel *KAT6A-LEUTX* fusion gene in a patient with therapy-related AML (FAB-M4) with t(8;19)(p11;q13). This is the sixth, but unique, *KAT6A* fusion partner which does not have a HAT domain (Fig. 5). Several previous studies have reported AML-M4 or M5 cases with t(8;19)(p11;q13) (Brizard et al., 1988; Stark et al., 1995), and a *KAT6A* rearrangement was detected

in an AML-M5 with t(8;19)(p11;q13) (Gervais et al., 2008), suggesting that this fusion is recurrent. To date, five genes have been identified as *KAT6A* fusion partners in translocations including *CREBBP*, *EP300*, *NCOA2*, *NCOA3*, and *ASXL2* in leukemia (GenBank accession no. AB084281) (Imamura et al., 2003) (Fig. 6). *LEUTX* and *ASXL2* differ from the other fusion partner genes, in terms of molecular characteristics. The remaining four have a histone acetyltransferase (HAT) domain, whereas *LEUTX* and *ASXL2* do not (Katoh and Katoh, 2004). *ASXL2* may theoretically interact with histone-modifying enzymes because its homolog is *ASXL1*, modulates the activity of *LSD1*, a histone demethylase of H3K4 and H3K9, by cooperation with heterochromatin protein-1 (*HP1*) (Wang et al., 2009; Lee et al., 2010). The sequence of the *LEUTX* gene contained in the *KAT6A-LEUTX* chimeric transcript is shorter than that of the other partner genes involved in *KAT6A* translocations, suggesting a different mechanism of leukemogenesis.

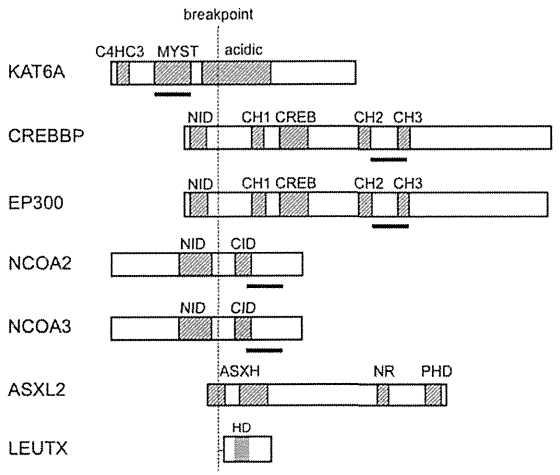

Figure 6. Schematic representation of putative KAT6A, LEUTX, and other KAT6A fusion proteins. C4HC3, zinc finger domain associated with chromatin binding; MYST, MYST domain; Acidic, Acidic domain; NID, nuclear hormone receptor interaction domain; CH 1–3, cysteine/histidine-rich domains 1–3; CREB, cyclic-AMP response element binding protein domain; CID, CBP-interacting domains; ASXH, ASX homology domain; NR, nuclear receptor box; PHD, plant homeodomain; HD, homeodomain; Horizontal bars, Regions of HAT domain.

LEUTX is characterized by the presence of a leucine residue at the otherwise highly conserved homeodomain position 20 (Holland et al., 2007). Although *LEUTX* is one of the homeobox genes, the translated protein has never been recorded in the NCBI database. However, *LEUTX* is potentially a protein-coding gene, based on previously reported findings. Firstly, *LEUTX* is highly conserved and necessary for placental mammals except rodents (Zhong and Holland, 2011). Secondly, the NCBI database now shows that *LEUTX* is expressed only in placental tissue. Our data by Northern blotting and RT-PCR also confirmed this. A previous report showed that thousands of genes are transcribed at a rate of only one copy per cell, yet do perform functions (Kuznetsov et al., 2002). These data strongly suggest that *LEUTX* is associated with the formation of the placenta. Thirdly, *LEUTX* is considered to arise by tandem duplication and extreme divergence from *CRX* (Zhong and Holland, 2011), which is a member of the *Otx* gene family interacting with *CREBBP*, *EP300*, and *NCOA2* (Yanagi et al., 2000), based on its localization close to the PRD-class genes *TPRX1*, *CRX*, *DPRX*, and *DUXA* on the distal end of the long arm of chromosome 19. These data suggest that *LEUTX* may function as a homeobox gene. Fourthly, a previous study of *NKX2.6* gene confirmed that the missense mutation of F151L at position 20 in the homeodomain reduced its transcriptional activation (Heathcote et al., 2005). This data suggests that leucine, but not phenylalanine, in LEUTX alters and reserves the transcriptional activity of the homeodomain protein. Finally, a KAT6A fusion partner *per se* may play a role in leukemogenesis, because a mutant KAT6A protein, transcribed from the truncated N-terminal part of KAT6A sequence within KAT6A-NCOA2, did not bind CREBBP in contrast to the full length KAT6A or KAT6A-NCOA2 protein in vitro (Collins et al., 2006).

```
                                  RNYNNCNNGYNGKTNYNY
                                  ******* ****** **
KAT6A          AAAATTTTAAGTTTTATGTTACGTATAGTTTACCATAGTTTTTTTAAAAATG
               ||||||||||||||||||||||||||
KAT6A-LEUTX    AAAATTTTAAGTTTTATGTTACGTAAAAGTCACTCATGCTAAATGCCACATT
                                          ||||||||||||||||||||||||||
LEUTX          CCAACGGACCAGACCAAACCAAAATAAAGTCACTCATGCTAAATGCCACATT
```

Figure 7. DNA sequences across the junction points of *KAT6A* and *LEUTX*. Topoisomerase II recognition site-like sequences (5′-RNYNNCNNGYNGKTNYNY-3′) near the junction points are aligned. R, purine; Y, pyrimidine; N, any base; K, G or T; and *, homology.

The patient in this study was exposed to pirarubicin for treatment of non-Hodgkin's lymphoma, which is associated with inactivation of topoisomerase II (TOPOII) and induction of DNA repair (Aplan et al., 1996). Analysis of the sequence around the genomic junction of *KAT6A-LEUTX* shows suggestive association with the TOPOII cleavage site (Fig. 7) (Spitzner and Muller, 1988). Furthermore, the breakpoint was located upstream of exon 1, though RT-PCR showed that exon 16 of *KAT6A* fused to exon 2 of *LEUTX* instead of exon 1. *KAT6A-LEUTX* fusion transcript containing the first exon of *LEUTX* could not be amplified in this case. Similar findings have been described, for example, the *ETV6-CDX2* fusion [t(12;13)(p13;q12)] in AML (Chase et al., 1999), *ETV6-GOT1* [t(10;12)(q24;p13)] in myelodysplastic syndrome (MDS) (Janssen et al., 2006), *MLL-GAS7* [t(11;17)(q23;p13)] in acute leukemia (Megonigal et al., 2000), *MLL-NCKIPSD* [t(3;11)(p21;q23)] in therapy-related AML (Sano et al., 2000), and *FUS-DDIT3* [t(12;16)(q13;p11)] in myxoid and round-cell liposarcoma (Kanoe et al., 1999) (Fig. 8). The 5′ side of the first exons are not flanked by splice recognition site; thus, the first exons in the 3′ side of genes would not be recognized as an exon in the mature fusion mRNA. Interestingly, in a case of MDS with t(10;12)(q24;p13)/*ETV6-GOT1*, a genomic region, which was located between the breakpoint at 10q24 and *GOT1*, created a fusion transcript with *ETV6* concurrently (Janssen et al., 2006).

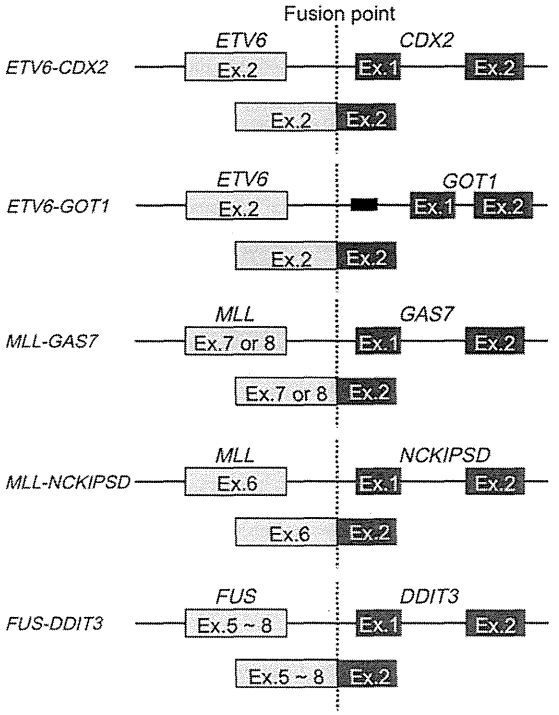

Figure 8. Schematic representation of several fusion transcripts with similar structures of the genomic junctions as in *KAT6A-LEUTX*. All five fusion genes have the genomic breakpoint 5′ upstream of first exons of 3′ side of fusion partners. Solid small box in *ETV6-GOT1*, a genomic region which created a fusion transcript with *ETV6* concurrently with *ETV6-GOT1* (Janssen et al., 2006).

Based on FAB classification, the subtype was defined as myelomonocytic in the present patient. *KAT6A*-related leukemias, except for those having *ASXL2* as a partner, are associated with the M4/M5, often therapy-related and with hemophagocytosis. In other AML cases with 8p11 translocations, including t(6;8)(q27;p11) (Brizard et al., 1988), t(3;8;17)(q27;p11;q12) (Bertheas et al., 1989), and t(8;14)(p11;q11.1) (Slovak et al., 1991), where the genes involved in these translocations have not been identified, the morphological phenotypes are highly similar to leukemias with *KAT6A* translocations (Table 2). Our case displayed an M4

TABLE 2. Summary of *KAT6A*-Related Hematologic Malignancies

Chromosome abnormality	Fusion partner	Phenotype	Clinical characteristics	Reference
t(8;16)(p11;p13)	*CREBBP*	AML-M4, M5	Therapy-related Hemophagocytosis	Borrow et al. (1996)
inv(8)(p11q13)	*NCOA2*	AML-M4, M5	Therapy-related Hemophagocytosis	Liang et al. (1998)
t(8;20)(p11;q13)	*NCOA3*	AML-M5	No hemophagocytosis	Esteyries et al. (2008)
t(8;22)(p11;q13)	*EP300*	AML-M4, M5	Therapy-related Hemophagocytosis	Chaffanet et al. (2000)
t(2;8)(p23;p11)	*ASXL2*	MDS	Therapy-related	Imamura et al. (2003)
t(8;19)(p11;q13)	*LEUTX*	AML-M4, M5	Therapy-related Hemophagocytosis	Present case Brizard et al. (1988) Stark et al. (1995); Gervais et al. (2008)
t(6;8)(q27;p11)	Unknown	AML-M5	Hemophagocytosis	Brizard et al. (1988)
t(3;8;17)(q27;p11;q12)	Unknown	AML-M5	Hemophagocytosis	Bertheas et al. (1989)
t(8;14)(p11;q11.1)	Unknown	AML-M5	Hemophagocytosis	Slovak et al. (1991)

phenotype, hemophagocytosis, and DIC, and other AML cases with t(8;19) also tend to have the M4/M5 phenotypes, hemophagocytosis, and DIC. Thus, the present case with t(8;19) is similar to other AML cases with *KAT6A* rearrangements.

In conclusion, *LEUTX* was identified as a *KAT6A* fusion partner. Molecular characterization of the *KAT6A-LEUTX* gene suggests that LEUTX may play a different role in leukemogenesis than other *KAT6A* partners previously identified.

ACKNOWLEDGMENTS

Authors wish to express their appreciation for the outstanding technical assistance of Minako Goto and Kayoko Kurita.

REFERENCES

Aguiar RC, Chase A, Coulthard S, Macdonald DH, Carapeti M, Reiter A, Sohal J, Lennard A, Goldman JM, Cross NC. 1997. Abnormalities of chromosome band 8p11 in leukemia: two clinical syndromes can be distinguished on the basis of MOZ involvement. Blood 90:3130–3135.

Aplan PD, Chervinsky DS, Stanulla M, Burhans WC. 1996. Site-specific DNA cleavage within the MLL breakpoint cluster region induced by topoisomerase II inhibitors. Blood 87:2649–2658.

Bertheas MF, Jaubert J, Vasselon C, Reynaud J, Pomier G, Le Petit JC, Hagemeijer A, Brizard CP. 1989. A complex t(3;8;17) involving breakpoint 8p11 in a case of M5 acute nonlymphocytic leukemia with erythrophagocytosis. Cancer Genet Cytogenet 42:67–73.

Borrow J, Stanton VP, Jr., Andresen JM, Becher R, Behm FG, Chaganti RS, Civin CI, Disteche C, Dubé I, Frischauf AM, Horsman D, Mitelman F, Volinia S, Watmore AE, Housman DE. 1996. The translocation t(8;16)(p11;p13) of acute myeloid leukaemia fuses a putative acetyltransferase to the CREB-binding protein. Nat Genet 14:33–41.

Brizard A, Guilhot F, Huret JL, Benz-Lemoine E, Tanzer J. 1988. The 8p11 anomaly in "monoblastic" leukaemia. Leuk Res 12: 693–697.

Chaffanet M, Gressin L, Preudhomme C, Soenen-Cornu V, Birnbaum D, Pébusque MJ. 2000. MOZ is fused to p300 in an acute monocytic leukemia with t(8;22). Genes Chromosomes Cancer 28:138–144.

Chase A, Reiter A, Burci L, Cazzaniga G, Biondi A, Pickard J, Roberts IA, Goldman JM, Cross NC. 1999. Fusion of ETV6 to the caudal-related homeobox gene CDX2 in acute myeloid leukemia with the t(12;13)(p13;q12). Blood 93:1025–1031.

Chinen Y, Taki T, Nishida K, Shimizu D, Okuda T, Yoshida N, Kobayashi C, Koike K, Tsuchida M, Hayashi Y, Taniwaki M. 2008. Identification of the novel AML1 fusion partner gene, LAF4, a fusion partner of MLL, in childhood T-cell acute lymphoblastic leukemia with t(2;21)(q11;q22) by bubble PCR method for cDNA. Oncogene 27:2249–2256.

Collins HM, Kindle KB, Matsuda S, Ryan C, Troke PJ, Kalkhoven E, Heery DM. 2006. MOZ-TIF2 alters cofactor recruitment and histone modification at the RARbeta2 promoter: differential effects of MOZ fusion proteins on CBP- and MOZ-dependent activators. J Biol Chem 281:17124–17133.

Esteyries S, Perot C, Adelaide J, Imbert M, Lagarde A, Pautas C, Olschwang S, Birnbaum D, Chaffanet M, Mozziconacci MJ. 2008. NCOA3, a new fusion partner for MOZ/MYST3 in M5 acute myeloid leukemia. Leukemia 22:663–665.

Gervais C, Murati A, Helias C, Struski S, Eischen A, Lippert E, Tigaud I, Penther D, Bastard C, Mugneret F, Poppe B, Speleman F, Talmant P, VanDen Akker J, Baranger L, Barin C, Luquet I, Nadal N, Nguyen-Khac F, Maarek O, Herens C, Sainty D, Flandrin G, Birnbaum D, Mozziconacci MJ, Lessard M; Groupe Francophone de Cytogénétique Hématologique. 2008. Acute myeloid leukaemia with 8p11 (MYST3) rearrangement: an integrated cytologic, cytogenetic and molecular study by the groupe francophone de cytogénétique hématologique. Leukemia 22:1567–1575.

Heathcote K, Braybrook C, Abushaban L, Guy M, Khetyar ME, Patton MA, Carter ND, Scambler PJ, Syrris P. 2005. Common arterial trunk associated with a homeodomain mutation of NKX2.6. Hum Mol Genet 14:585–593.

Holland PW, Booth HA, Bruford EA. 2007. Classification and nomenclature of all human homeobox genes. BMC Biol 5:47.

Huntly BJ, Shigematsu H, Deguchi K, Lee BH, Mizuno S, Duclos N, Rowan R, Amaral S, Curley D, Williams IR, Akashi K, Gilliland DG. 2004. MOZ-TIF2, but not BCR-ABL, confers properties of leukemic stem cells to committed murine hematopoietic progenitors. Cancer Cell 6:587–596.

Imamura T, Kakazu N, Hibi S, Morimoto A, Fukushima Y, Ijuin I, Hada S, Kitabayashi I, Abe T, Imashuku S. 2003. Rearrangement of the MOZ gene in pediatric therapy-related myelodysplastic syndrome with a novel chromosomal translocation t(2;8)(p23;p11). Genes Chromosomes Cancer 36:413–419.

Janssen H, Wlodarska I, Mecucci C, Hagemeijer A, Vandenberghe P, Marynen P, Cools J. 2006. Fusion of ETV6 to GOT1 in a case with myelodysplastic syndrome and t(10;12)(q24;p13). Haematologica 91:949–951.

Kanoe H, Nakayama T, Hosaka T, Murakami H, Yamamoto H, Nakashima Y, Tsuboyama T, Nakamura T, Ron D, Sasaki MS, Toguchida J. 1999. Characteristics of genomic breakpoints in TLS-CHOP translocations in liposarcomas suggest the involvement of Translin and topoisomerase II in the process of translocation. Oncogene 18:721–729.

Katoh M, Katoh M. 2004. Identification and characterization of ASXL3 gene in silico. Int J Oncol 24:1617–1622.

Katsumoto T, Aikawa Y, Iwama A, Ueda S, Ichikawa H, Ochiya T, Kitabayashi I. 2006. MOZ is essential for maintenance of hematopoietic stem cells. Genes Dev 20:1321–1330.

Kuznetsov VA, Knott GD, Bonner RF. 2002. General statistics of stochastic process of gene expression in eukaryotic cells. Genetics 161:1321–1332.

Lee SW, Cho YS, Na JM, Park UH, Kang M, Kim EJ, Um SJ. 2010. ASXL1 represses retinoic acid receptor-mediated transcription through associating with HP1 and LSD1. J Biol Chem 285:18–29.

Liang J, Prouty L, Williams BJ, Dayto MA, Blanchard KL. 1998. Acute mixed lineage leukemia with an inv(8)(p11q13) resulting in fusion of the genes for MOZ and TIF2. Blood 92:2118–2122.

Megonigal MD, Cheung NK, Rappaport EF, Nowell PC, Wilson RB, Jones DH, Addya K, Leonard DG, Kushner BH, Williams TM, Lange BJ, Felix CA. 2000. Detection of leukemia-associated MLL-GAS7 translocation early during chemotherapy with DNA topoisomerase II inhibitors. Proc Natl Acad Sci USA 97:2814–2819.

Paggetti J, Largeot A, Aucagne R, Jacquel A, Lagrange B, Yang XJ, Solary E, Bastie JN, Delva L. 2010. Crosstalk between leukemia-associated proteins MOZ and MLL regulates HOX gene expression in human cord blood CD34+ cells. Oncogene 29:5019–5031.

Patnaik MM, Gangat N, Knudson RA, Keefe JG, Hanson CA, Pardanani A, Ketterling RP, Tefferi A. 2010. Chromosome 8p11.2 translocations: Prevalence, FISH analysis for FGFR1 and MYST3, and clinicopathologic correlates in a consecutive cohort of 13 cases from a single institution. Am J Hematol 85: 238–242.

Sano K, Hayakawa A, Piao JH, Kosaka Y, Nakamura H. 2000. Novel SH3 protein encoded by the AF3p21 gene is fused to the mixed lineage leukemia protein in a therapy-related leukemia with t(3;11) (p21;q23). Blood 95:1066–1068.

Slovak ML, Nemana L, Traweek ST, Stroh JA. 1991. Acute monoblastic leukemia (FAB-M5b) with t(8;14)(p11;q11.1). Cancer Genet Cytogenet 56:237–242.

Smith DR. 1992. Ligation-mediated PCR of restriction fragments from large DNA molecules. PCR Methods Appl 2:21–27.

Spitzner JR, Muller MT. 1988. A consensus sequence for cleavage by vertebrate DNA topoisomerase II. Nucleic Acids Res 16: 5533–5556.

Stark B, Resnitzky P, Jeison M, Luria D, Blau O, Avigad S, Shaft D, Kodman Y, Gobuzov R, Ash S, Stein J, Yaniv I, Barak Y, Zaivov R. 1995. A distinct subtype of M4/M5 acute myeloblastic leukemia (AML) associated with t(8:16)(p11:p13), in a patient with the variant t(8:19)(p11:q13)-case report and review of the literature. Leuk Res 19:367–379.

Taniwaki M, Matsuda F, Jauch A, Nishida K, Takashima T, Tagawa S, Sugiyama H, Misawa S, Abe T, Kashima K. 1994. Detection of 14q32 translocations in B-cell malignancies by in situ hybridization with yeast artificial chromosome clones containing the human IgH gene locus. Blood 83:2962–2969.

Thomas T, Corcoran LM, Gugasyan R, Dixon MP, Brodnicki T, Nutt SL, Metcalf D, Voss AK. 2006. Monocytic leukemia zinc finger protein is essential for the development of long term reconstituting hematopoietic stem cells. Genes Dev 20:1175–1186.

Wang J, Hevi S, Kurash JK, Lei H, Gay F, Bajko J, Su H, Sun W, Chang H, Xu G, Gaudet F, Li E, Chen T. 2009. The lysine demethylase LSD1 (KDM1) is required for maintenance of global DNA methylation. Nat Genet 41:125–129.

Yanagi Y, Masuhiro Y, Mori M, Yanagisawa J, Kato S. 2000. p300/CBP acts as a coactivator of the cone-rod homeobox transcription factor. Biochem Biophys Res Commun 269:410–414.

Zhang JG, Goldman JM, Cross NC. 1995. Characterization of genomic BCR-ABL breakpoints in chronic myeloid leukaemia by PCR. Br J Haematol 90:138–146.

Zhong YF, Holland PW. 2011. The dynamics of vertebrate homeobox gene evolution: gain and loss of genes in mouse and human lineages. BMC Evol Biol 11:169.

Identification of novel fusion genes with 28S ribosomal DNA in hematologic malignancies

SATORU KOBAYASHI[1], TOMOHIKO TAKI[2], HISAO NAGOSHI[1], YOSHIAKI CHINEN[1], YUICHI YOKOKAWA[2], HIROKAZU KANEGANE[3], YOSUKE MATSUMOTO[1], JUNYA KURODA[1], SHIGEO HORIIKE[1], KAZUHIRO NISHIDA[1] and MASAFUMI TANIWAKI[1]

Departments of [1]Molecular Hematology and Oncology and [2]Molecular Diagnostics and Therapeutics, Kyoto Prefectural University of Medicine Graduate School of Medical Science, Kyoto; [3]Department of Pediatrics, Graduate School of Medicine and Pharmaceutical Sciences, University of Toyama, Toyama, Japan

Received December 4, 2013; Accepted January 2, 2014

DOI: 10.3892/ijo.2014.2291

Abstract. Fusion genes are frequently observed in hematologic malignancies and soft tissue sarcomas, and are usually associated with chromosome abnormalities. Many of these fusion genes create in-frame fusion transcripts that result in the production of fusion proteins, and some of which aid tumorigenesis. These fusion proteins are often associated with disease phenotype and clinical outcome, and act as markers for minimal residual disease and indicators of therapeutic targets. Here, we identified the 28S ribosomal DNA (*RN28S1*) gene as a novel fusion partner of the B-cell leukemia/lymphoma 11B gene (*BCL11B*), the immunoglobulin κ variable 3-20 gene (*IGKV3-20*) and the component of oligomeric Golgi complex 1 gene (*COG1*) in hematologic malignancies. The *RN28S1-BCL11B* fusion transcript was identified in a case with mixed-lineage (T/myeloid) acute leukemia having t(6;14)(q25;q32) by cDNA bubble PCR using *BCL11B* primers; however, the gene fused to *BCL11B* on 14q32 was not on 6q25. *IGKV3-20-RN28S1* and *COG1-RN28S1* fusion transcripts were identified in the Burkitt lymphoma cell line HBL-5, and the multiple myeloma cell line KMS-18. *RN28S1* would not translate, and the breakpoints in partner genes of *RN28S1* were within the coding exons, suggesting that disruption of fusion partners by fusion to *RN28S1* is the possible mechanism of tumorigenesis. Although further analysis is needed to elucidate the mechanism(s) through which these *RN28S1*-related fusions play roles in tumorigenesis, our findings provide important insights into the role of rDNA function in human genomic architecture and tumorigenesis.

Correspondence to: Dr Tomohiko Taki, Department of Molecular Diagnostics and Therapeutics, Kyoto Prefectural University of Medicine Graduate School of Medical Science, 465 Kajii-cho Kawaramachi-Hirokoji, Kamigyo-ku, Kyoto 602-8566, Japan
E-mail: taki-t@umin.net

Key words: 28S ribosomal DNA, RN28S1, fusion transcript, BCL11B, IGK, COG1, leukemia, lymphoma, multiple myeloma

Introduction

Fusion genes are frequently observed in hematologic malignancies and soft tissue sarcomas (1). These fusion genes are usually associated with chromosome abnormalities such as translocations, inversions, and deletions, but have also been identified in cryptic chromosome abnormalities. Fusion genes have also been identified in various solid tumors, including *ETS*-family fusion genes in prostate cancer (2), *ETV6-NTRK3* in secretory breast cancer (3), and *ALK* fusion genes in lung cancer (4). Many of these fusion genes create in-frame fusion transcripts that result in the production of fusion proteins, and some of which aid tumorigenesis. These fusion proteins are often associated with disease phenotype and clinical outcome, and act as markers for minimal residual disease and indicators of therapeutic targets. However, several fusion genes that do not create in-frame fusion transcripts have also been identified. Oncogenic rearrangements of immunoglobulin (*IG*) or T-cell receptor (*TCR*) genes are well-known fusion genes, and some of these create fusion transcripts, such as *IGH-BACH2* by t(6;14)(q15;q32) in B-cell lymphoma/leukemia (5), *IGH-MMSET* by t(4;14)(p16.3;q32.3) (6) and *Cα-IRTA1* by t(1;14)(q21;q32) (7) in multiple myeloma, and *BCL11B-TRDC* by inv(14)(q11.2q32.31) in T-cell acute lymphoblastic leukemia (8). Furthermore, chromosome abnormalities led to fusion transcripts in the non-coding gene *PVT1* such as *PVT1-NBEA* and *PVT1-WWOX* in multiple myeloma (9), *PVT1-CHD7* in small-cell lung carcinoma (10), and *PVT1-MYC* and *PVT1-NDRG1* in medulloblastoma (11). The role of *PVT1*-fusions is uncertain, but they may represent another type of fusion transcript in cancer cells and possibly in normal cells.

In the present study, we unexpectedly identified additional fusion genes involving 28S ribosomal DNA (*RN28S1*) in hematologic malignancies.

Materials and methods

Clinical sample and cell lines. Leukemic cells from a 15-year-old boy with mixed-lineage (T/myeloid) acute leukemia having t(6;14)(q25;q32) were analyzed after obtaining informed consent from the patient's parents. In

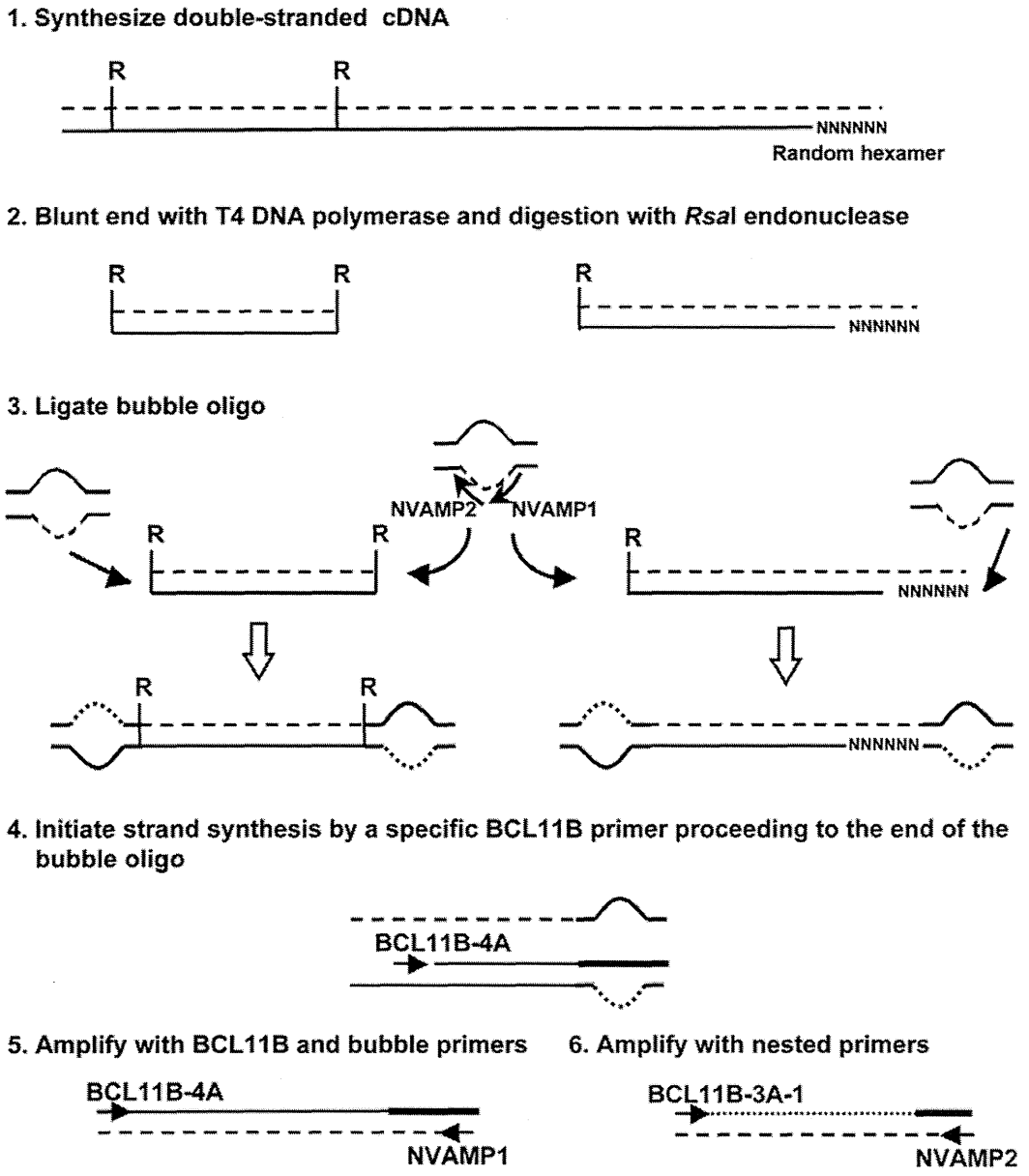

Figure 1. Outline of cDNA bubble PCR method used for the detection of *RN28S1-BCL11B* fusion transcript.

addition, 14 B-cell non-Hodgkin's lymphoma, 11 multiple myeloma, 4 B-cell precursor acute lymphoblastic leukemia cell lines, and 3 EB virus-transformed B-cell lines from normal healthy volunteers were analyzed; the cell lines were as described previously (5). The Institutional Review Board of Kyoto Prefectural University of Medicine approved this study.

cDNA bubble PCR. cDNA bubble PCR was used to detect the fusion partner of *BCL11B*, as described previously (Fig. 1) (12). Total RNA was used to generate double-stranded cDNA. Primers used were: NVAMP-1 and BCL11B-4A for first-round PCR, and NVAMP-2 and BCL11B-3A-1 for second-round PCR (Fig. 1 and Table I).

Reverse transcription (RT)-PCR. RT-PCR analysis was performed as described previously (5). Primers used for the detection of *BCL11B-RN28S1* fusion transcripts were BCL11B-3A-2 and RN28S1-GA1 for first-round PCR, and BCL11B-3A-1 and RN28S1-GA2 for second-round PCR; those for *IGKV3-20-RN28S1* were IGKV3-20-2F and

Table I. Primers used for PCR.

Primer	Sequence 5'-3'
BCL11B-3A-1	ACGCAGAGGTGAAGTGATCAC
BCL11B-3A-2	GACAACTGACACTGGCATCC
BCL11B-4A	ACCACGCGCTGTTGAAGGG
RN28S1-GA1	CCTTAGCGGATTCCGACTTCCAT
RN28S1-GA2	GTCCTGCTGTCTATATCAACCAACAC
IGKV3-20-2F	GGCTCCTCATCTATGGTGCATC
COG1-11F	AACAGCAACCTTCATCGCCTG

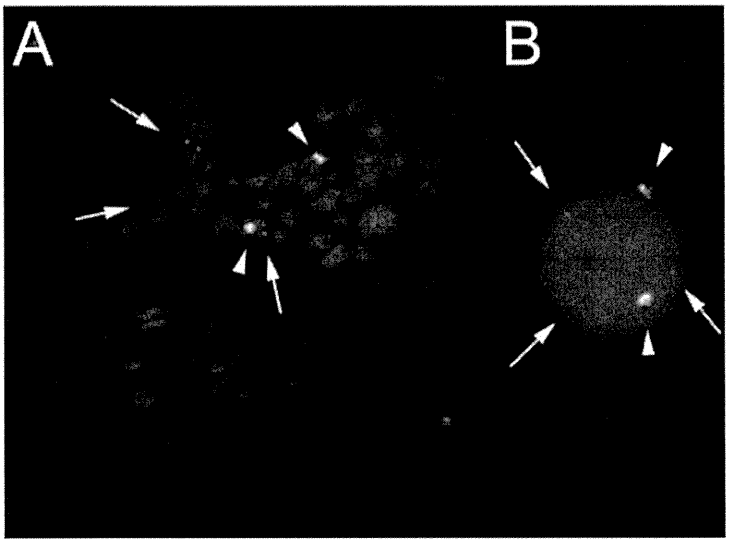

Figure 2. Fluorescence *in situ* hybridization analysis of the leukemic metaphase (A) and interphase (B). Split signals of BAC clone, RP11-431B1 (red, arrows), that encompassed *BCL11B* gene on 14q32, were detected. Arrowheads indicate CEP6 probe (centromere of chromosome 6, green).

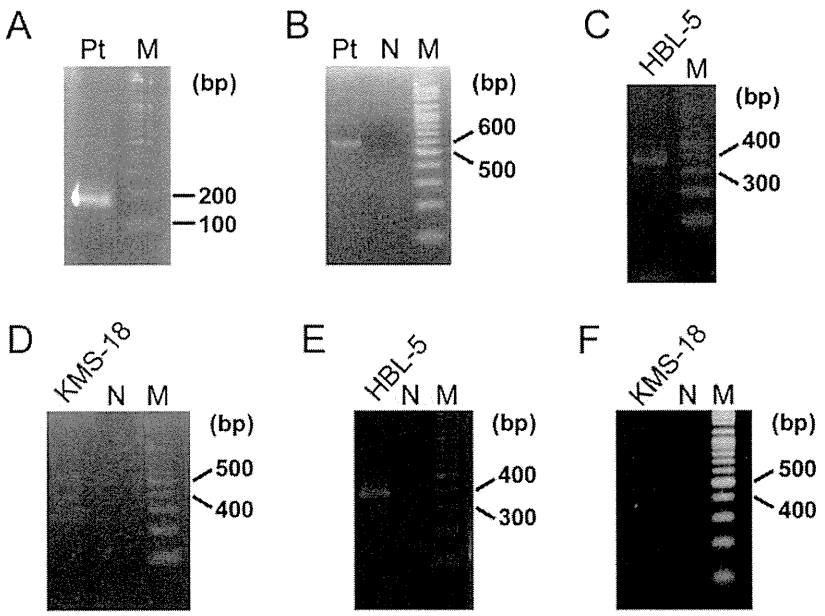

Figure 3. Identification of *BCL11B-RN28S1*, *IGKV3-20-RN28S1* and *COG1-RN28S1* fusion transcripts. (A) Bubble PCR products from a mixed-lineage acute leukemia patient sample. (B) Confirmation of *BCL11B-RN28S1* fusion transcript by nested RT-PCR. Detection of *IGKV3-20-RN28S1* fusion transcript (C) and multiple amplicons including *COG1-RN28S1* fusion transcript (D) by nested RT-PCR for the detection of *BCL11B-RN28S1*. RT-PCR using specific primers confirmed *IGKV3-20-RN28S1* (E) and *COG1-RN28S1* (F) fusion transcripts. Lanes are: Pt, mixed-lineage acute leukemia patient; N, negative control (water); M, size marker.

RN28S1-GA1; and those for *COG1-RN28S1* were COG1-11F and RN28S1-GA1 (Table I).

Nucleotide sequencing. Nucleotide sequences of PCR products and, if necessary, subcloned PCR products were analyzed as previously described (5).

Results

Identification of RN28S1-BCL11B fusion transcript by cDNA bubble PCR method. Leukemic cells from a patient with mixed-lineage acute leukemia having t(6;14)(q25;q32) were analyzed using fluorescence *in situ* hybridization analysis, and rearrangement of the B-cell leukemia/lymphoma 11B (*BCL11B*) gene was suggested (Fig. 2). Thus, we performed cDNA bubble PCR to identify the gene on chromosome 6q25 that was fused to the *BCL11B* gene on 14q32. Sequence analysis of multiple products amplified by second-round PCR of bubble PCR detected a product that contained a 34-bp sequence of *BCL11B* exon 3 fused to an unknown 96-bp sequence (Fig. 3A). A BLAST search revealed that the unknown sequence was 28S ribosomal DNA (*RN28S1*)

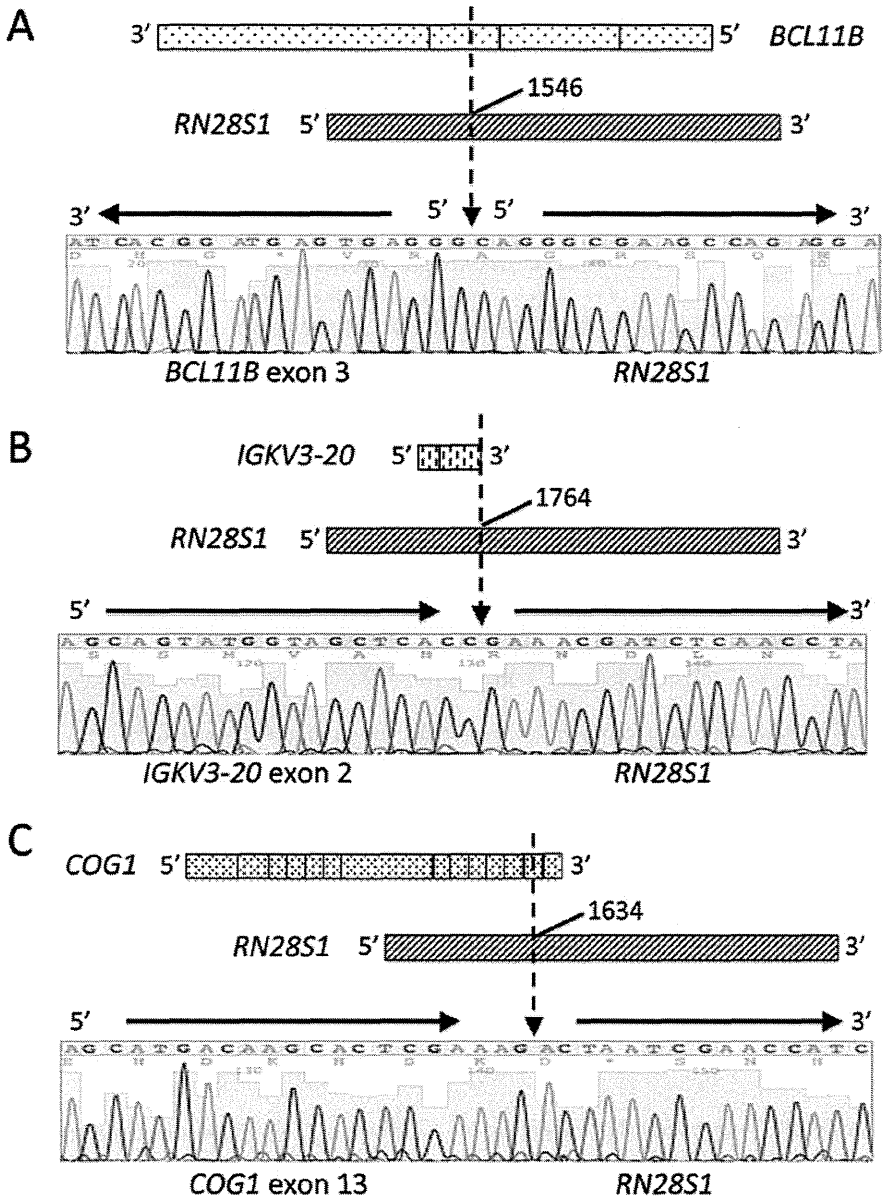

Figure 4. Structure of three fusion transcripts of *RN28S1*. (A) *BCL11B-RN28S1*. (B) *IGKV3-20-RN28S1*. (C) *COG1-RN28S1*. Dashed arrows indicate fusion points. Horizontal arrows indicate transcriptional orientation.

(Fig. 4A). This fusion transcript was confirmed by RT-PCR (Fig. 3B). The transcriptional directions of the contributing genes in the fusion transcript were opposed, and the fusion point of *BCL11B* was within the exon (Fig. 4A). No sequences from chromosome 6q25 were identified.

Accidental detection of IGK-RN28S1 and COG1-RN28S1 fusion transcripts in B-cell malignancy cell lines. *RN28S1* is one of three ribosomal DNAs encoding the 18S, 5.8S and 28S rRNAs, which exist in nucleolar organizer regions on the five acrocentric chromosomes (13p, 14p, 15p, 21p and 22p). Therefore, in this case, the *RN28S1-BCL11B* fusion transcript was considered not to be generated by the chromosome translocation of t(6;14)(q25;q32). Thus, we could infer that a mechanism other than chromosome abnormalities was involved in the creation of the *RN28S1-BCL11B* fusion transcript. To analyze whether the *RN28S1-BCL11B* fusion transcripts were expressed in other hematologic malignancy cell lines, RT-PCR using *RN28S1* and *BCL11B* primers was performed. PCR products were detected in several cell lines. In the Burkitt lymphoma cell line HBL-5, a 367-bp PCR product (Fig. 3C), contained 119-bp of immunoglobulin κ variable 3-20 (*IGKV3-20*) exon 2 fused to an *RN28S1* sequence (Fig. 4B). The multiple myeloma cell line KMS-18, amplified multiple PCR products (Fig. 3D) including a 441-bp product that resulted from a 62-bp sequence of the component of oligomeric Golgi complex 1 (*COG1*) gene fused to an *RN28S1* sequence (Fig. 4C). These fusions both occurred within the exons of *IGKV3-20* and *COG1*, as in the *RN28S1-BCL11B* fusion, and they were confirmed by RT-PCR using each specific primer (Fig. 3E and F).

Comparison of the sequence of BCL11B primer with those of *IGKV3-20* and *COG1* found similarities between them, with

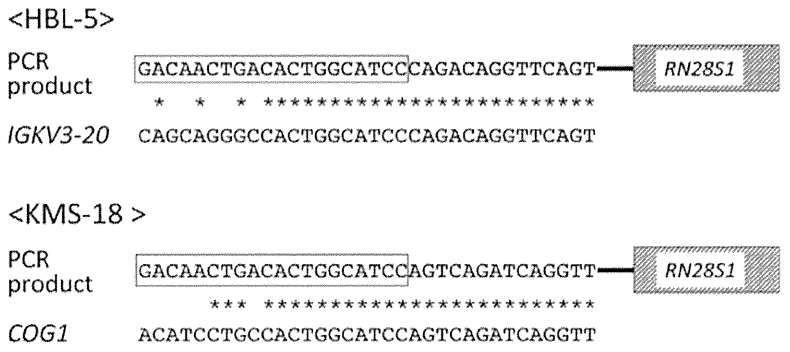

Figure 5. Comparison of nucleotide sequences of *BCL11B* primer and those of *IGKV3-20* and *COG1*. Primer BCL11B-3A-1 is boxed. *Identity.

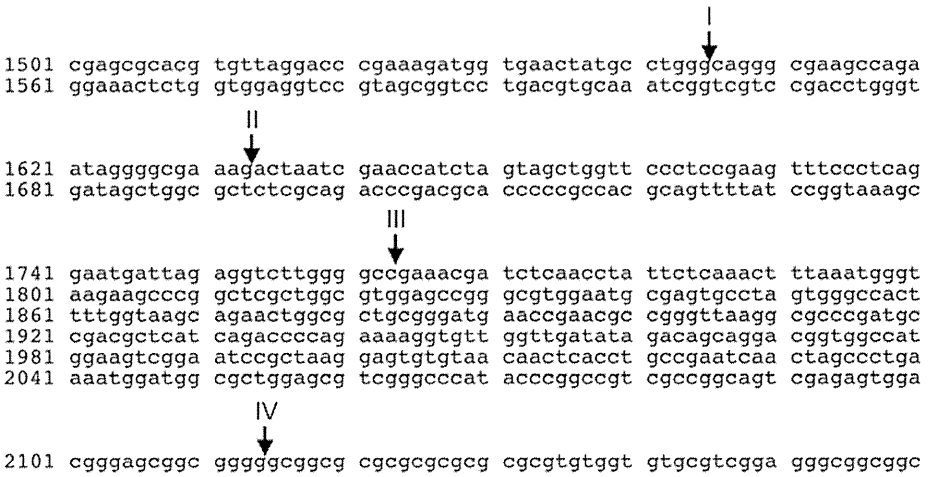

Figure 6. Breakpoint cluster region within *RN28S1*. Nucleotides are numbered (left side of the sequence) according to GenBank accession NR_003287. Vertical arrows indicate the breakpoints in cases with *BCL11B-RN28S1* (I), *COG1-RN28S1* (II), *IGKV3-20-RN28S1* (III) and *BCL-6-RN28S1* (IV). Three MYC binding sites are at positions 1344-1349, 1507-1521 (relates to the coanonical pathway) and 3655-3661 (relate to non-canonical pathway).

six mismatches in 20 nucleotides, suggesting that annealing of the primer to the similar sequences of *IGK* and *COG1* made it possible to amplify these fusion genes by chance (Fig. 5). Other products amplified by RT-PCR for the detection of *RN28S1-BCL11B* were either the normal sequence of *RN28S1* or non-specific sequences.

Discussion

In the present study, we identified three novel fusion transcripts involving *RN28S1*. Only one *RN28S1*-related fusion gene, *RN28S1-BCL6*, has been previously reported, and this was in a case of gastric lymphoma (13). *RN28S1* is a gene that would not translate to protein, and the breakpoints in partner genes of *RN28S1* were within the coding exons. Notably, *BCL11B* and *RN28S1* were fused with opposite transcription directions. These findings suggest that fusion genes involving *RN28S1* do not produce fusion proteins, but that disruption of the normal functions of fusion partners contribute to tumorigenesis in these cases.

Several studies have noted an association of ribosomal DNA (RNA) with tumorigenesis. rRNA transcription and ribosome biogenesis are controlled by several cancer-related genes through the PI3 kinase/mTOR, MYC or RAS/ERK pathways (14). Proto-oncoprotein MYC controls ribosome biogenesis through the regulation of transcription by all three RNA polymerases (15). Another cancer-related gene, nucleophosmin (*NPM1*), which is frequently mutated in acute myeloid leukemia with a normal karyotype and creates fusion genes with *ALK* in anaplastic large cell lymphoma with t(2;5)(p23;q35), is necessary for MYC-mediated rRNA synthesis (16). *RN28S1* has three MYC-binding sites (17), and the breakpoints within *RN28S1* in our cases were to the 5' side of the MYC-binding sites (Fig. 6), suggesting that the *RN28S1*-fusion transcripts we detected are associated with tumorigenesis through the dysregulation of MYC-mediated rRNA synthesis. In other correlations of rDNA with tumorigenesis, a high frequency of rDNA rearrangements was noted in lung and colon cancers (18) and overexpression of rDNA was seen in prostatic cancer (19). The breakpoints of *RN28S1* in our three cases were within an ~600 bp region (Fig. 6); these may be related to recombinational hot spots in repetitive sequences.

The three genes fused to *RN28S1* that we found in our study are related to tumorigenesis in certain types of malignancies. *IGK* is one of the immunoglobulin light chain genes that is frequently rearranged by chromosome translocations, such as t(2;8)(p11;q24) in B-cell malignancies (20). Rearrangement of the *BCL11B* gene locus is observed in T-cell

malignancies, and three fusion transcripts involving *BCL11B* have been identified: *TLX3-BCL11B* fusion gene by cryptic t(5;14)(q35;q32.2) in T-ALL (21), *BCL11B-TRDC* by inv(14)(q11.2q32.31) in T-ALL (8) and *HELIOS-BCL11B* by t(2;14)(q34;q32) in adult T-cell leukemia (22). *COG1* is a component of the conserved oligomeric Golgi (COG) complex, Golgi transport complex, that is involved in glycosylation reactions and vesicular transport (23). Although the *COG1* gene has not been firmly associated with tumorigenesis to date, one *COG* family gene, *COG5*, was found fused to *HMGA2* in uterine leiomyoma (24), suggesting a possible link with tumorigenesis. Although the fusion genes we identified in this study were not related to chromosome translocations, each gene is involved in tumorigenesis in some way, suggesting that *RN28S1*-related fusion genes play some roles in tumorigenesis.

Molecular analysis of ribosomal DNA is challenging due to its repetitive nature. In this study, we attempted to confirm the three fusions at the genomic level; however, genomic PCR was unsuccessful. A possible explanation for the failure of amplification of genomic junctions is the quantitative imbalance of genomic DNAs between partner genes and *RN28S1* due to the ~400 copies of ribosomal DNA in a diploid human genome. Whole-transcriptome analysis by next-generation sequencing is usually a powerful tool for the detection of fusion transcripts. However, detection of *RN28S1* fusion transcripts using this method is difficult, because ribosomal RNAs, which comprises >95% of total RNA, is usually removed from total RNA prior to sequencing. While further analysis is needed to clarify the role of rDNA in tumorigenesis, our findings provide an important insight into the role of rDNA function in human genomic architecture and tumorigenesis.

Acknowledgements

We express appreciation to Akari Kazami for the outstanding technical assistance. This study was supported by a research program of the Project for Development of Innovative Research on Cancer Therapeutics (P-Direct), a Grant-in-Aid for Cancer Research from the Ministry of Health, Labor and Welfare of Japan, and a Grant-in-Aid for Scientific Research (C) from the Ministry of Education, Culture, Sports, Science and Technology of Japan.

References

1. Taki T and Taniwaki M: Chromosomal translocations in cancer and their relevance for therapy. Curr Opin Oncol 18: 62-68, 2006.
2. Tomlins SA, Rhodes DR, Perner S, *et al*: Recurrent fusion of TMPRSS2 and ETS transcription factor genes in prostate cancer. Science 310: 644-648, 2005.
3. Euhus DM, Timmons CF and Tomlinson GE: ETV6-NTRK3 - Trk-ing the primary event in human secretory breast cancer. Cancer Cell 2: 347-348, 2002.
4. Soda M, Choi YL, Enomoto M, *et al*: Identification of the transforming EML4-ALK fusion gene in non-small-cell lung cancer. Nature 448: 561-566, 2007.
5. Kobayashi S, Taki T, Chinen Y, *et al*: Identification of IGHCδ-BACH2 fusion transcripts resulting from cryptic chromosomal rearrangements of 14q32 with 6q15 in aggressive B-cell lymphoma/leukemia. Genes Chromosomes Cancer 50: 207-216, 2011.
6. Chesi M, Nardini E, Lim RS, Smith KD, Kuehl WM and Bergsagel PL: The t(4;14) translocation in myeloma dysregulates both FGFR3 and a novel gene, MMSET, resulting in IgH/MMSET hybrid transcripts. Blood 92: 3025-3034, 1998.
7. Hatzivassiliou G, Miller I, Takizawa J, *et al*: IRTA1 and IRTA2, novel immunoglobulin superfamily receptors expressed in B cells and involved in chromosome 1q21 abnormalities in B cell malignancy. Immunity 14: 277-289, 2001.
8. Przybylski GK, Dik WA, Wanzeck J, *et al*: Disruption of the BCL11B gene through inv(14)(q11.2q32.31) results in the expression of BCL11B-TRDC fusion transcripts and is associated with the absence of wild-type BCL11B transcripts in T-ALL. Leukemia 19: 201-208, 2005.
9. Nagoshi H, Taki T, Hanamura I, *et al*: Frequent PVT1 rearrangement and novel chimeric genes PVT1-NBEA and PVT1-WWOX occur in multiple myeloma with 8q24 abnormality. Cancer Res 72: 4954-4962, 2012.
10. Pleasance ED, Stephens PJ, O'Meara S, *et al*: A small-cell lung cancer genome with complex signatures of tobacco exposure. Nature 463: 184-190, 2010.
11. Northcott PA, Shih DJ, Peacock J, *et al*: Subgroup-specific structural variation across 1,000 medulloblastoma genomes. Nature 488: 49-56, 2012.
12. Chinen Y, Taki T, Nishida K, *et al*: Identification of the novel AML1 fusion partner gene, LAF4, a fusion partner of MLL, in childhood T-cell acute lymphoblastic leukemia with t(2;21)(q11;q22) by bubble PCR method for cDNA. Oncogene 27: 2249-2256, 2008.
13. Chen YW, Hu XT, Liang AC, *et al*: High BCL6 expression predicts better prognosis, independent of BCL6 translocation status, translocation partner, or BCL6-deregulating mutations, in gastric lymphoma. Blood 108: 2373-2383, 2006.
14. Montanaro L, Treré D and Derenzini M: Changes in ribosome biogenesis may induce cancer by down-regulating the cell tumor suppressor potential. Biochim Biophys Acta 1825: 101-110, 2012.
15. Dai MS and Lu H: Crosstalk between c-Myc and ribosome in ribosomal biogenesis and cancer. J Cell Biochem 105: 670-677, 2008.
16. Li Z and Hann SR: Nucleophosmin is essential for c-Myc nucleolar localization and c-Myc-mediated rDNA transcription. Oncogene 32: 1988-1994, 2013.
17. Grandori C, Gomez-Roman N, Felton-Edkins ZA, *et al*: c-Myc binds to human ribosomal DNA and stimulates transcription of rRNA genes by RNA polymerase I. Nat Cell Biol 7: 311-318, 2005.
18. Stults DM, Killen MW, Williamson EP, *et al*: Human rRNA gene clusters are recombinational hotspots in cancer. Cancer Res 69: 9096-10104, 2009.
19. Uemura M, Zheng Q, Koh CM, Nelson WG, Yegnasubramanian S and De Marzo AM: Overexpression of ribosomal RNA in prostate cancer is common but not linked to rDNA promoter hypomethylation. Oncogene 31: 1254-1263, 2012.
20. Croce CM and Nowell PC: Molecular basis of human B cell neoplasia. Blood 65: 1-7, 1985.
21. MacLeod RA, Nagel S, Kaufmann M, Janssen JW and Drexler HG: Activation of HOX11L2 by juxtaposition with 3'-BCL11B in an acute lymphoblastic leukemia cell line (HPB-ALL) with t(5;14)(q35;q32.2). Genes Chromosomes Cancer 37: 84-91, 2003.
22. Fujimoto R, Ozawa T, Itoyama T, Sadamori N, Kurosawa N and Isobe M: HELIOS-BCL11B fusion gene involvement in a t(2;14)(q34;q32) in an adult T-cell leukemia patient. Cancer Genet 205: 356-364, 2012.
23. Ungar D, Oka T, Brittle EE, *et al*: Characterization of a mammalian Golgi-localized protein complex, COG, that is required for normal Golgi morphology and function. J Cell Biol 157: 405-415, 2002.
24. Velagaleti GV, Tonk VS, Hakim NM, *et al*: Fusion of HMGA2 to COG5 in uterine leiomyoma. Cancer Genet Cytogenet 202: 11-16, 2010.